A Positron Study of Early Clustering in Al-Mg-Si Alloys

Meng Liu[1,a] [*], Jakub Čížek[3,b], Cynthia S. T. Chang[2,c], and John Banhart[1,2,d]

[1]Helmholtz-Zentrum Berlin (HZB), Hahn-Meitner-Platz 1, D-14109 Berlin, Germany

[2]Technische Universität Berlin, Hardenbergstr. 36, D-10623 Berlin, Germany

[3]Charles University in Prague, V Holešovičkách 2, CZ-18000 Praha 8, Czech Republic

[a]meng.liu@helmholtz-berlin.de, [b]jakub.cizek@mff.cuni.cz, [c]cynthia.chang@helmholtz-berlin.de, [d]john.banhart@tu-berlin.de

Keywords: Al-Mg-Si, Natural ageing, Vacancy, Solute cluster, Positron annihilation.

Abstract. Early stages of clustering in quenched Al-Mg-Si alloys during natural ageing (NA) were studied by positron annihilation lifetime spectroscopy (PALS) utilizing its unique sensitivity to electron density differences in various atomic defects. Two different positron trapping sites could be identified, one related to a vacancy-type defect, the other to solute clusters. The first trap is deep, i.e. irreversibly traps positrons, the second shallow, from which positrons can escape, which creates the signature of a temperature-dependent positron lifetime. During the first 80 min of NA, the vacancy-related contribution decreases, while the solute clusters increasingly trap positrons, thus reflecting their continuous growth and power to trap positrons. Coincident Doppler broadening spectroscopy (CDBS) of the annihilation radiation shows that the annihilation sites are Si-rich after quenching but contain more Mg after 80 min.

Introduction

It is known that age-hardenable Al-Mg-Si alloys can be strengthened through the formation of solute clusters during NA at 'room temperature' (RT) and precipitates upon artificial aging (AA). The clusters formed during NA can positively or negatively influence subsequent AA which is of great practical relevance and therefore motivates to study NA in more detail. Atom probe tomography, although useful for analyzing small objects such as clusters, is currently too slow to resolve clustering kinetics and also a reliable detection of clusters is challenging.

Integral techniques such as hardness or resistivity measurement, thermoanalysis and positron annihilation spectroscopy have demonstrated that clustering in Al-Mg-Si alloys is a complex multi-stage process. In particular, by using positron annihilation lifetime spectroscopy (PALS), it could be shown that the evolution of positron lifetime (LT) in Al-Mg-Si alloys involves at least 4 stages, i.e. a stage I of nearly constant LT, a stage II of decrease, a stage III of increase and, finally, another decrease in stage IV [1]. In order to further clarify the underlying microscopic processes behind these stages, samples naturally aged for different times after quenching are characterised at low temperatures in PALS spectrometers with a time resolution sufficient to distinguish between different LT components and therefore different positron annihilation sites. In addition, the chemical environment of the annihilation site was further identified by coincidence Doppler broadening spectroscopy, which utilizes the positron sensitivity to the momentum distribution of annihilating electrons.

Experiments

Samples. A ternary Al-0.45at.%Mg-0.38at.%Si alloy of designation 'H' (also used in [1]) was cast, homogenized, extruded to 3 mm and cold rolled to 1 mm by Hydro Aluminium. 10 mm×10 mm-large platelets, 1-mm thick for PALS and CDBS were used. The samples were solutionised at ~540 ℃ for 1 h and then quenched into ice water, after which they were cleaned, dried, assembled
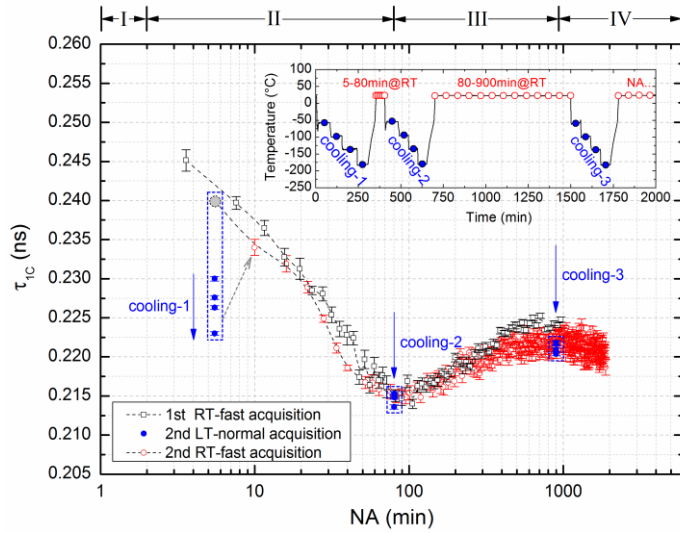
Figure 1: Single-component lifetime (τ_{1C}) evolution during NA of one sample measured at RT – 1st run, black open symbols – and the temperature dependence of positron lifetime in selected NA states – 2nd run, measured at low temperatures (blue) and LT in between at RT (red). Grey point is estimate of lifetime for the sample aged for 5 min at RT. The insert explains the temperature profile. At the top, the four observed stages are marked I to IV in accordance with [1].

with the positron emitter to the required sandwich geometry and rapidly placed into the sample holder. The total delay from quenching to measurement including the time for evacuation and cooling was equivalent to ~5 min of NA. In-situ PALS measurements (see Fig. 1) were sequentially performed at various low temperatures to avoid any undesired microstructural changes. Data were collected at each temperature with sufficient statistics. After this, samples were heated up to RT and NA for a given time there, after which the cooling and measuring procedure was repeated. In this way, various NA states were investigated. For the results shown in Fig. 2 and 3, different samples were aged at RT for various periods and then cooled down and measured by PALS or CDBS.

PALS. The positron lifetime can be measured as the time difference between the 1.27 MeV γ emission almost simultaneously emitted with a positron and one of the 0.511 MeV emissions indicating annihilation of the positron.

At the analog PALS spectrometer of HZB, the positron source contained ~20 μCi ^{22}Na enclosed by a 7.5-μm thick Kapton foil. The sandwich containing both the samples and source was placed into a holder with temperature control inside a vacuum chamber. Both detectors were arranged closely in 180° geometry in order to ensure a high count rate. The parasite back scattering problem from this alignment was settled by inserting a 7-mm lead shield in front of the start detector. A count rate of ~800 s^{-1} and a time resolution of 0.22 ns can be achieved. The data were either accumulated for good statistics or evaluated in the fast acquisition mode [2].

PALS measurements were also performed at Charles University in Prague where a very high time resolution (0.145 ns) of a digital spectrometer [3] allows to accurately separate LT components. Here, a ^{22}Na positron source with an activity of 27 μCi was sealed between 2-μm thick Ti foils. To reduce back-scattering, the sandwich was moved out of the common axis to a radial distance slightly higher than the radius of the BaF$_2$ scintillators [4]. During positron lifetime measurements the samples were kept at a temperature of −150 °C. At least 5×10^6 counts were accumulated in each spectrum. Source contributions and background contributions were subtracted from the positron lifetime spectra for measurements at both spectrometers.

CDBS. The momentum of the annihilation (e$^+$, e$^-$) pair is transferred to the annihilation γ quanta. The component p_L in the propagation direction of the two quanta is distributed symmetrically around the annihilation peak at 0.511 MeV. Many events add up to a symmetrical broadening of the annihilation peak. The chemical surroundings of the annihilation sites can be probed by measuring the high-momentum distribution of the core electrons. By measuring in coincidence with two detectors, not only the background can be markedly reduced by at least two orders of magnitude, but also the energy resolution can be improved by a factor of ~1.4 [5]. For in-situ CDBS experiments, samples aged for ~5 min and ~80 min were measured at −150 °C at Charles University in Prague

directly after PALS measurement. Two Ortec coaxial HPGe detectors and the 27-μCi ^{22}Na sources were used. The spectrometer has a coincidence count rate of ~600 s^{-1} and an energy resolution of ~1.0 keV. The evaluation of the momentum distribution was carried out by dividing the data by the distribution of a well-annealed aluminium reference sample (6N). By doing this, any annihilation component not related to Al bulk gives rise to a signal which differs from unity.

Results and Discussion

Single-Component PALS Analysis. The course of the one-component LT of alloy H during NA is known from previous studies and shows distinct stages, see Fig. 1, namely an initial stage II, where the lifetime decreases from ~0.245 ns to ~0.215 ns within ~80 min, followed by stage III, a slow increase to 0.222 ns until ~900 min, and finally stage IV, where the LT decrease slowly again. The existence of a very short (less than 2 min@RT) and slight increase in stage I can be best observed at low temperatures or in alloy with a higher Mg and Si content [1]. The main focus of this study was put on the ageing kinetics during stage II, namely, from ~5 min to ~80 min after quenching.

A different temperature dependence of positron lifetime in various states of ageing was observed. For the sample NA for 5 min, LT is markedly reduced from ~0.24 ns at RT to ~0.223 ns at −180 °C during cooling sequence 1. After 80 min and 935 min of NA (cooling sequence 2 and 3), this dependence largely disappeared. This tendency is in agreement with a previous study [6].

The temperature dependence after 5 min of NA, points at the existence of 'shallow traps', which compete with the 'deep positron traps' (1–2 eV) related to quenched-in vacancies. Such shallow traps could be small solute clusters in which positrons have lifetimes well above bulk aluminium. At RT, the weak binding energies of positron and shallow trap (~typically 30–40 meV) are insufficient to trap positrons since their thermal energies are of the same order and thus they easily de-trap and barely contribute to annihilation. But when temperature and positron energies decrease, more and more positrons will be localized at the shallow traps (which become relatively deeper) due to the decrease of de-trapping. Under such circumstances, the increasing fraction of positron annihilating in the shallow traps faster than in vacancies notably affects the observed lifetime τ_{1C}, which can be roughly approximated as the weighted sum of each of the individual lifetime components:

$$\tau_{1c} \approx \bar{\tau} = \tau_f \cdot I_f + \tau_s \cdot I_s + \tau_v \cdot I_v , \tag{1}$$

where $\bar{\tau}$ is the average positron lifetime, τ_f, τ_s and τ_v represent the decomposed lifetimes of **f**ree positrons, **s**olute clusters and **v**acancy-related defects, I_f, I_s, and I_v denote the corresponding intensities. τ_f is also called the 'reduced bulk lifetime' since it is shorter than the lifetime of a positron in pure aluminium bulk.

During subsequent NA, solute clusters increase in their geometrical sizes and after certain ageing time, they could not be further regarded as 'shallow traps', since positrons eventually get trapped by these clusters even at RT, as a result of the increase in their positron binding energies. Under such circumstances, a much weaker temperature dependence of τ_{1C} is expected, as compared to the one after 5 min of NA. Combining all lifetime components and applying Eq.(1), the different types of temperature dependencies of τ_{1C} can be explained. In order to verify this explanation, the parameters in Eq.(1) need to be determined.

Multi-Component PALS Analysis. Owing to the excellent time resolution of the spectrometer (0.145 ns) at Charles University in Prague, three distinct lifetime components could be resolved during stage II without fixing any of the fitting parameters in Eq.(1). The up to three lifetimes τ_i found are shown in Fig. 2 as a function of their corresponding intensities I_i:
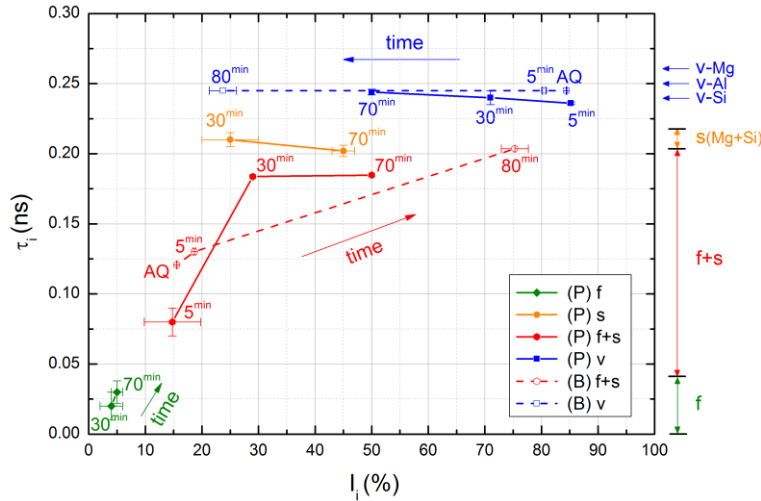
Figure 2: Evolution of decomposed positron lifetime components during stage II. Lifetimes as a function of intensities are given. Measurements labelled with '(P)' and solid symbols were performed at the Uni. Prague, while data labelled with '(B)' and open symbols show experiments conducted at HZB using the same alloy. On the right, the lifetimes in some vacancy-related defects as well as the range of reduced lifetimes in clusters and bulk Al are shown. Unlike in Fig. 1, each point corresponds to a newly quenched sample.

The vacancy-related long life-time component (blue solid square) varies from 0.236 to 0.245 ns, slightly shorter than the lifetime in a mono-vacancy in Al, and can be attributed to positrons trapped by vacancy-Si complexes since Si is expected to decrease the LT of a positron trapped in a Al-vacancy, while Mg acts in the opposite direction [7,8]. This interpretation is supported by the high jump frequency of vacancies decorated with Si, which is ~100 times higher than for Mg [9]. Moreover, it is known from binary Al-0.5at.%Mg alloys [2] that unlike in Al-Si no vacancy agglomeration takes place, i.e. the mono-vacancy – mostly attached to a solute – is 'stabilized' by the presence of Mg

[10]. Certainly, the long lifetime component could also be related to positron trapping in solute clusters other than those characterized by lifetime τ_s. For example cluster atoms that do not occupy substitutional sites one-to-one but leave some open volume could give rise to a lifetime τ_v as well. During NA, I_v is significantly lowered from 85% to 50%, indicating a decreasing contribution of the associated defects to total lifetime. Elimination of vacancies at sinks and vacancies trapped inside certain solute clusters could be responsible for this decrease in intensity, but such a decrease would be accompanied by an increase of a bulk component which we do not observe. More likely, the decrease of I_v is caused by the formation and growth of coherent clusters enriched in Mg and/or Si in which the positrons have a LT τ_s ranging from 0.2 to 0.21 ns (see orange symbols). This lifetime is much shorter than τ_v and implies that these clusters are vacancy-free. Therefore, identifying them with the shallow traps already detected is near at hand. By neglecting the interactions between solutes, the total vacancy concentration after quenching in an Al-Mg-Si alloy can be estimated to 1.42×10^{-4}/atom employing Lomer's equation [11], but the actual vacancy concentration should be even less due to the loss of vacancies during and after quenching. Therefore, a solute/vacancy ratio of >100 is realistic. In this case, even if each cluster consisted of 10 solute atoms (which is realistic in view of atom probe data), there will be still >10 times more clusters than vacancies and >90% of clusters would be vacancy-free. Upon NA, these clusters gradually replace vacancy-containing defects in trapping positrons provided that a critical radius is exceeded, which can be estimated from the positron affinities of Mg (–6.18eV), Si (–6.95eV) and Al (–4.41eV). For example, the critical radius of Si precipitates is $r_{c-Si} = 5.8\,\text{Å}/\sqrt{\Delta A[eV]} = 3.8\,\text{Å}$ [12], where ΔA is the difference in positron affinity between Si and Al. Si has an atomic radius of 1.46 Å, indicating that already few Si atoms in a cluster are able to localize positrons. For Mg, the situation is similar.

The shortest lifetime component (green diamonds) contributes only weakly to LT. It originates from free positron annihilation in the Al bulk. This component can be distinguished in samples aged for 30 min and 80 min, but not for 5 min. In order to facilitate discussion, we combine the contribution of free positrons and the solute cluster component to τ_{f+s}:

$$\tau_{f+s} = \tau_f \cdot \frac{I_f}{I_f + I_s} + \tau_s \cdot \frac{I_s}{I_f + I_s}, \quad \text{and } I_{f+s} = I_f + I_s. \tag{2}$$

Based on this equation, the weighted sum of the free positron and the solute cluster contributions was plotted in Fig. 2 (red solid hexagon), showing that both lifetime and intensity increase continuously during NA. Such a feature was also found from the experiments carried out at HZB using the same alloy. The rationale for additional experiments was to include an experiment for the as-quenched state (AQ) where natural ageing after quenching could be suppressed by quenching to $<-100\,^{\circ}$C and always keeping the sample at low temperature after. Instead of decomposing the lifetime spectra into 3 components, only a two- components analysis was applied to the spectra measured at $-60\,^{\circ}$C due to the limited time resolution of the employed spectrometer. In addition, the longer lifetime component representing the vacancy-related defects was fixed to 0.245 ns to minimize statistical uncertainties from fitting. Results are given in Fig. 2 as open symbols. The two data sets for the two spectrometers show the same trend, but differ in two details: (1) for 30 min of NA, τ_{f+s} (P) is much higher than τ_{f+s} (B), this might be caused by the much lower measuring temperature of $-150\,^{\circ}$C rather than $-60\,^{\circ}$C. Localization of positrons by shallow traps (solute clusters) will be enhanced at cooling and therefore the Mg signature will appear stronger due to the Mg content of the clusters. (2) the ageing kinetics of the alloy measured at Prague appears slower, e.g. after 80 min of NA, the intensity I_{f+s} (P) is just 50%, which is 25% lower than I_{f+s} (B). This could be due to a higher quenching rate at HZB, giving rise to more efficient solute clustering.

CDBS Ratio Curve Analysis. The Si ratio curve exhibits two peaks located at $p \approx 3$ and 8×10^{-3} m_0c. On the other hand, the ratio curve for pure Mg is characterized by a pronounced minimum at $p \approx 7 \times 10^{-3}$ m_0c followed by a local maximum located at $p \approx 11 \times 10^{-3}$ m_0c. One can see in Fig. 3 that the ratio curves for alloy H measured after 5 min of NA exhibit a peak at $p \approx 8 \times 10^{-3}$ m_0c, which is a signature for positrons annihilated by electrons at Si sites or in vacancies in Al. Actually the high momentum part ($p > 15 \times 10^{-3}$ m_0c) of the ratio curve is almost identical with that for pure Si. This testifies that defects in quenched alloys are surrounded mainly by Si atoms. Hence, shortly (here ~5 min) after quenching positrons are trapped mostly by vacancy-Si complexes. Inspection of Fig. 3 further shows that the peak at $p \approx 8 \times 10^{-3}$ m_0c is lower in the alloy aged for 70 min at RT. This indicates a decrease in the contribution of positrons annihilated by electrons at Si sites. Thus, the relative contribution to annihilation of vacancy-Si complexes decreases in accordance with a decrease in the intensity of the component with lifetime $\tau_v \approx 0.24$ ns observed by PALS. This is accompanied by an enhancement in the high-momentum range suggesting a rising contribution of positrons annihilated by electrons at Mg sites. This is plausible since the appearance of coherent clusters characterized by a lifetime $\tau_s \approx 0.21$ ns has been detected by PALS already and these clusters certainly contain Mg and Si solutes. As after 70-80 min of NA between 50 and 75% of the annihilation take place in such clusters there must be a considerable amount of Mg in these vacancy-free clusters. This finding differs from a measurement in previous

Figure **3**: CDBS ratio plots of alloy H aged for 5 min and 70 min at RT. The ratio curves for reference samples of pure Si (6N) and pure Mg (4N) are plotted as well.

work, where the signal remained dominated by Si sites even after long NA. This discrepancy could be due to the different alloy used, the higher measurement temperature and/or the different measurement method applied there [13].

Summary

The ageing kinetics of an Al-0.45%Mg-0.38%Si alloy was studied using positron annihilation techniques, it was found that:
1. Shallow positron traps exist during the initial stage of NA as verified by temperature-dependent PALS experiments and applying a single-component analysis. These are identified as vacancy-free coherent solute clusters.
2. Multi-components PALS analysis in 3 stages of NA shows different types of competing positron annihilation sites including vacancy-free clusters and solute-vacancy complexes.
3. CDBS experiments demonstrate that after quenching Si-V complexes dominate, but that during the first 80 min of natural ageing clusters form that include Mg atoms beside Si.
4. The three positron annihilation experiments carried out yield a consistent picture of the phenomena during early clustering during NA.

Acknowledgments

References

[1] J. Banhart, M.D.H. Lay, C.S.T. Chang, A.J. Hill, Phys. Rev. B, 83 (2011) 014101.

[2] M. Liu, Y. Yan, Z.Q. Liang, C.S.T. Chang, J. Banhart, Proceedings of ICAA-13, Eds.: H. Weiland, A.D. Rollett, W.A. Cassada, TMS and Wiley, (2012) 1131-1137.

[3] F. Bečvář, J. Čížek, I. Procházka, J. Janotová, Nucl. Instrum. Methods A, 539 (2005) 372-385.

[4] F. Bečvář, J. Čížek, L. Lešták, I. Novotný, I. Procházka, F. Šebesta, Nucl. Instrum. Methods A, 443 (2000) 557-577.

[5] R. Krause-Rehberg, Positron Annihilation in Semi-Conductors, Springer (2003) pp.19.

[6] B. Klobes, PhD thesis, University of Bonn (2010) 101.

[7] C. Corbel, R.P. Gupta, J. Phys. Lett. 42 (1981) 549.

[8] O. Melikhova, J. Kuriplach, J. Cizek, I. Prochazka, Appl. Surf. Sci. 252 (2006) 3288.

[9] Z.Q. Liang, C.S.T. Chang, C. Abromeit, J. Banhart, J. Hirsch, Int. J. Mat. Res. 103 (2012) 980.

[10] A. Somoza, M. P. Petkov, K. G. Lynn, Phys. Rev. B 65 (2002) 094107.

[11] W.M. Lomer, Monograph Rept. Ser. Vol. 23, The Institute of Metals London, (1958) 79.

[12] M.J. Puska, R.M. Nieminen, J. Phys. 1 (1989) 6091.

[13] J. Banhart, M. Liu, Y. Yan, Z. Liang, C.S.T. Chang, M. Elsayed, M.D.H. Lay, Physica B 407 (2012) 2689.